Letter

Relevance of on-site and intersite Coulomb interactions in the Kitaev-Heisenberg magnet $Na_3Co_2SbO_6$

Pritam Bhattacharyya [1,2,3,*] Abdul Basit,[4] Thorben Petersen [1] Stephan Rachel,[4] Satoshi Nishimoto [1,5] and Liviu Hozoi[1,†]

[1]*Institute for Theoretical Solid State Physics, Leibniz IFW Dresden, Helmholtzstraße 20, 01069 Dresden, Germany*

[2]*Department of Physics, Karpagam Academy of Higher Education, Coimbatore 641021, Tamil Nadu, India*

[3]*Centre for Computational Physics, Karpagam Academy of Higher Education, Coimbatore 641021, Tamil Nadu, India*

[4]*School of Physics, University of Melbourne, Parkville, Victoria 3010, Australia*

[5]*Department of Physics, Technical University Dresden, 01069 Dresden, Germany*

(Received 1 March 2026; accepted 9 March 2026; published 1 April 2026)

The detection of considerable spin frustration in honeycomb cobalt oxide compounds indicates the presence of sizable Kitaev interactions in these systems, enlarging the pool of Kitaev spin liquid candidates. Several key questions remain to be answered, as basic as the mechanisms behind Kitaev couplings in Co^{2+} $t_{2g}^5e_g^2$ magnets. Analyzing the quantum chemistry of interacting magnetic moments in $Na_3Co_2SbO_6$, a representative *LS*-coupled $t_{2g}^5e_g^2$ oxide, we find that the Kitaev and off-diagonal Γ interactions are substantial and antiferromagnetic but somewhat weaker than the Heisenberg contribution. All nearest-neighbor couplings feature massive contributions from direct Coulomb exchange and/or on-site multiconfigurational dressing, mechanisms not considered so far in descriptive models of Kitaev-Heisenberg magnetism. These findings call for systematic wave function quantum chemical studies to understand direct-indirect exchange synergies in Kitaev-Heisenberg magnets and how to possibly tune intersite couplings toward the Kitaev spin liquid ground state.

DOI: 10.1103/8fz7-9wj9

Introduction. Science relies on models. First hypothesized, then tested, a model may later turn out to be valid or inadequate. Atomic models, for example, have undergone many changes over time, culminating in the quantum theory of atoms. Famed byproducts of the latter are the notions of spin and exchange.

Exchange is ubiquitous in electronic matter. It can be direct, as inferred in the 1920s, but also indirect, i.e., proceeding through interatomic charge transfer (CT). The functions of magnetic materials in technological applications rely on exchange.

Exchange can be isotropic as in Heisenberg magnets or, when spin-orbit couplings (SOCs) are present, highly anisotropic as in Ising or more recently identified Kitaev magnetic systems. Proposed initially as an exactly soluble magnetic model, Kitaev's construct [1] became a major reference point in condensed matter magnetism. It is of interest not only as fundamental research but also for possible applications in quantum technologies.

Direct Coulomb exchange is computed exactly in *ab initio* wave function-based quantum chemistry [2,3] but not in density functional theory (DFT) simulations that rely on functionals typically employed in solid-state physics, local density and generalized gradient functionals. In current descriptive magnetic interaction models, direct Coulomb exchange is ignored—not only for the case of edge-sharing Kitaev-Heisenberg magnets [4–11], but also in, e.g., edge-sharing cuprate chains, another class of emblematic frustrated magnets. Direct Coulomb exchange is of particular relevance to edge-sharing connectivity since certain pairs of metal (M) *d* orbitals are in 'direct contact' through the space left 'empty' between the two bridging ligands (Ls), different from corner-sharing ML_6 octahedra and linear M-L-M bonds.

As for excitations, i.e., L $\rightarrow$M CT (i.e., superexchange) and M $\rightarrow$M CT (hopping-mediated kinetic exchange): those do not explicitly enter canonical DFT. In a non-DFT context, analytical work based on simplified valence-band effective CT models and second-order perturbation theory may (i) imply remarkable intuition, (ii) reveal fascinating new physics, and (iii) open up exciting new research avenues; this was indeed the case with the initial *LS*-coupled, CT valence-band model (and analysis) of Khaliullin and Jackeli [4,5]. Yet, there is room (or even the need) for investigations beyond effective CT valence-band models and simple, perturbation-theory expressions. Further, if we want to understand the interplay of indirect CT exchange and direct Coulomb exchange, we need to put both into the same machinery; as pointed out above, only the quantum chemical computational machinery is presently able to describe both CT excitations and direct exchange.

Here, we pin down the underlying exchange mechanisms in $Na_3Co_2SbO_6$, a honeycomb cobaltate whose macroscopic magnetic properties indicate substantial frustration

*Contact author: pritambhattacharyya01@gmail.com

†Contact author: l.hozoi@ifw-dresden.de

Published by the American Physical Society under the terms of the Creative Commons Attribution 4.0 International license. Further distribution of this work must maintain attribution to the author(s) and the published article's title, journal citation, and DOI.

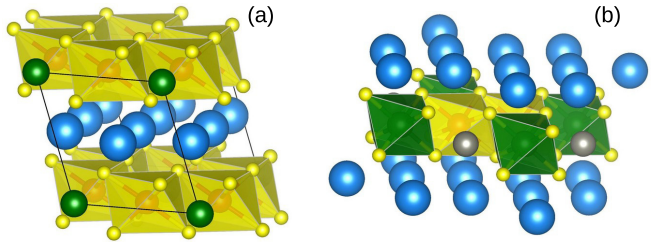


FIG. 1. (a) Successive atomic layers in $Na_3Co_2SbO_6$. The CoO_6 octahedra are represented in yellow; Na and Sb species are shown in blue and green, respectively. Each Sb sits in the center of a hexagonal ring formed by Co ions. (b) Cluster employed for deriving the nearest-neighbor effective magnetic couplings. The SbO_6 octahedra are highlighted in green. The embedding is not pictured. A different perspective is provided in the Supplemental Material [22].

[12–15], presumably arising from sizable, bond-dependent [5,7] anisotropic intersite interactions. We first demonstrate the capabilities of our quantum chemical methodology by scanning the many-body Co-site multiplet structure, benchmarked against existing inelastic neutron scattering (INS) measurements [13] and analysis of x-ray spectra [16]. Focusing then on intersite effective couplings, we unveil the morphology of Co-Co anisotropic exchange: important nearest-neighbor interaction mechanisms turn out to be direct Coulomb exchange and dressing with on-site excitations, according to the quantum chemical data. This physics has been largely overlooked in current descriptive electronic models of Kitaev-Heisenberg magnetism. Our findings call for a re-evaluation of the global landscape of symmetric anisotropic pseudospin interactions in quantum materials.

Co-site multiplet structure. The distribution of the different atomic species in $Na_3Co_2SbO_6$ is illustrated in Fig. 1. The Co^{2+} magnetic ions form a honeycomb network. The valence electronic structure of the Co^{2+} magnetic centers, as obtained by *ab initio* quantum chemical analysis, is detailed in Table I. Here, we built on insights gained from quantum chemical investigations of a series of other cobaltates, d^6 [17], d^7 [18], and d^8 [19]. Various features concerning the Co-ion ground state and multiplet structure can be directly compared with information extracted from spectroscopic investigations already carried out on $Na_3Co_2SbO_6$: the degree of $t_{2g}^5e_g^2$-$t_{2g}^4e_g^3$ configurational mixing in the ground-state wave function [16], the trigonal splitting of the Co $3d$ t_{2g} levels δ [16], and the position of the low-lying '$LS\delta$' exciton [13].

To disentangle crystal-field effects, on-site Coulomb interactions, and SOCs, embedded-cluster quantum chemical calculations were first performed at the single-configuration (SC) $t_{2g}^5e_g^2$ level, i.e., excluding other orbital occupations [see Supplemental Material (SM) for computational details] [22]. SC results are provided in the first column of Table I: it is seen that the $^4T_{1g}$ $(t_{2g}^5e_g^2)$ manifold is split by trigonal and residual lower-symmetry [21] fields into distinct components. By allowing subsequently for all possible orbital occupations within the Co $3d$ shell, which is referred to as complete-active-space self-consistent-field (CASSCF) [2,23], an admixture of 8% $t_{2g}^4e_g^3$ character is found in the ground-state CASSCF wave function, in agreement with conclusions drawn from the analysis of x-ray spectra [16]. Interestingly, given the low point-group symmetry [21], the $t_{2g}^5e_g^2$-$t_{2g}^4e_g^3$ interaction implies also Coulomb matrix elements that in cubic environment are 0 by symmetry: the trigonal splitting within the $^4T_{1g}$ manifold is consequently reduced from a bare value of 100 meV (SC results in Table I) to 60 meV (CASSCF data)—while $^4T_{1g}(t_{2g}^5e_g^2)$–$^4T_{1g}(t_{2g}^4e_g^3)$ interaction occurs already in the cubic environment, differential effects may appear within the group of 'initial' T_{1g} levels in symmetry lower than O_h. Such physics has yet to be discussed in effective-model theory [8,10,11,13,16]. Significantly heavier 'dressing' may occur in the case of multi-M-site, molecular-like $j \approx 1/2$ [24] and $j \approx 3/2$ [25] spin-orbit states, up

TABLE I. Co^{2+} $3d^7$ multiplet structure in $Na_3Co_2SbO_6$. SC stands for a single-configuration $(t_{2g}^5e_g^2)$ $S = 3/2$ calculation. Each value in the last two columns indicates a Kramers doublet (KD); for the ^4T terms, the KDs are listed as groups of closely spaced states. Only states with relative energies lower than 2 eV are listed. Notations as in O_h symmetry are used [20], though the actual point-group symmetry is lower [21].

Relative energies (eV)	SC	CASSCF[a]	CASSCF+SOC[b]	MRCI+SOC
$^4T_{1g}$ $(t_{2g}^5e_g^2)$	0	0[c]	0[d]	0
	0.10	0.06	0.03, 0.07 [e]	0.03[f], 0.07
	0.11	0.06	0.13, 0.14, 0.15[g]	0.13, 0.13, 0.15
$^4T_{2g}$ $(t_{2g}^4e_g^3)$[h]		0.85	0.81, 0.82	0.88, 0.89
		0.87	0.84, 0.85, 0.86	0.91, 0.91, 0.92
		0.88	0.88	0.94
$^4A_{2g}$ $(t_{2g}^3e_g^4)$		1.83	1.72, 1.72	1.77, 1.83
^2E_g $(t_{2g}^6e_g^1)$			1.93, 1.98	1.85, 1.85

[a]Orbitals optimized for the lowest three $S = 3/2$ roots; the SC splittings in the adjacent column are obtained using this orbital basis.
[b]Orbitals optimized for all $S = 3/2$ and the lowest 20 (out of 50) $S = 1/2$ roots; all $S = 3/2$ and the lowest 20 $S = 1/2$ $3d^7$ states were included in the spin-orbit treatment, at both CASSCF and MRCI levels.
[c]8% $t_{2g}^4e_g^3$ character, as also estimated by van Veenendaal *et al.* [16] from the analysis of x-ray spectra.
[d]0.33% admixture of excited state configurations through second-order SOCs.
[e]$j = 3/2$ quartet in cubic symmetry.
[f]$j = 5/2$ sextet in cubic symmetry.
[g]The $^4T_{1g}$ $(t_{2g}^4e_g^3)$ levels lie at 2.9–3.05 eV.
[h]27.5 meV, in agreement with the experimentally observed exciton at 28–29 meV [13].

to the point where the picture of 'dressing' even breaks down [25].

Upon including SOCs, at either CASSCF or multireference configuration-interaction (MRCI) [2,26] level, additional splittings occur. The lowest on-site excitation is computed at 27.5 meV (see footnote f in Table I), in excellent agreement with the outcome of INS measurements [13]. It is seen that, for the lower part of the spectrum, the MRCI corrections to the CASSCF relative energies are moderate.

Magnetic interactions. For a block of two adjacent edge-sharing ML_6 octahedra in layered honeycomb magnets, the highest possible point-group symmetry is C_{2h}. This implies a generalized bilinear effective spin Hamiltonian of the following form for a pair of adjacent 1/2-pseudospins $\tilde{\mathbf{S}}_i$ and $\tilde{\mathbf{S}}_j$:

$$\mathcal{H}_{ij}^{(\gamma)} = J\tilde{\mathbf{S}}_i \cdot \tilde{\mathbf{S}}_j + K\tilde{S}_i^{\gamma}\tilde{S}_j^{\gamma} + \sum_{\alpha\neq\beta}\Gamma_{\alpha\beta}\left(\tilde{S}_i^{\alpha}\tilde{S}_j^{\beta} + \tilde{S}_i^{\beta}\tilde{S}_j^{\alpha}\right). \quad (1)$$

The $\Gamma_{\alpha\beta}$ coefficients denote the off-diagonal components of the 3×3 symmetric-anisotropy exchange tensor, with $\alpha, \beta, \gamma \in \{x, y, z\}$. For, e.g., a z-type M-M bond (i.e., M_2L_2 plaquette normal to the z axis), $\Gamma \equiv \Gamma_{xy}$ and $\Gamma' \equiv \Gamma_{yz} = \Gamma_{zx}$.

Several studies of the INS spectra of $Na_3Co_2SbO_6$ arrive at antiferromagnetic Kitaev coupling K [13] plus sizable, antiferromagnetic off-diagonal Γ [13,15], and indicate that an antiferromagnetic K requires ferromagnetic Heisenberg interaction with $K \sim |J|$ [14], although fits with ferromagnetic K are also available [13,14]. In fact, a ferromagnetic-K model can lead to the identical magnon spectrum as an antiferromagnetic-K model [14,27]. That is, fitting an effective model to the experiment has limited evidential value. A relatively large ferromagnetic Heisenberg J is also proposed by analysis of effective models relying on Co-Co kinetic exchange, Co-O_2-Co superexchange, and intersite hoppings extracted from DFT computations [10].

For an *ab initio* quantum chemical perspective, we scanned the nearest-neighbor interaction landscape at the SC (i.e., $t_{2g}^5e_g^2$-$t_{2g}^5e_g^2$ Co nearest neighbors, no excited-state configurations considered), CASSCF, and MRCI levels (see SM [22] for technicalities). This allows us to distinguish between (i) direct, Coulomb exchange (the only available channel at SC level), (ii) Co-Co kinetic exchange (additionally accounted for in the CASSCF computation with all 3d orbitals of the two Co sites considered in the active space), and (iii) Co-O_2-Co superexchange (physics considered by MRCI). Remarkably, for J, K, and Γ, we find that CASSCF (i.e., CT kinetic exchange) and MRCI (CT superexchange) bring only minor corrections to the SC values (see Table II).

Also interesting is the effect of on-site excitations, i.e., the admixture of $t_{2g}^4e_g^3$ character to the leading Co^{2+} $t_{2g}^5e_g^2$ electron configuration (also discussed in the previous section), on Γ'. As shown on the second line of Table II and in Fig. 2, this on-site multiconfigurational 'dressing' reverts the sign of Γ', from ferromagnetic at the SC level to antiferromagnetic by single-site complete-active-space (SSCAS) multiconfiguration calculations where Co-Co hopping is excluded. The sign of Γ' remains then positive (i.e., antiferromagnetic) when including additional electronic excitations in the CASSCF and MRCI spin-orbit computations (the lowest two lines in Table II). It turns out that, compared to the SC calculation, on-site Coulomb matrix elements considered in the SSCAS numerical experiment modify the sequence of two of the four eigenstates in the two-site magnetic problem. This is how the sign of Γ' changes.

TABLE II. Magnetic couplings (meV) for the C_{2h} Co-Co link [21]. The singlet, triplet, quintet, and septet associated with each of the possible (3 × 3) $t_{2g}^5e_g^2$-$t_{2g}^5e_g^2$ orbital occupations were included in the spin-orbit treatment, which yields 144 spin-orbit states; the lowest four were mapped onto the model of two interacting 1/2 pseudospins (1), as described in [28,29]. SSCAS stands for single-site complete-active-space (Co–Co CT excluded); all possible d-d excitations, on-site + intersite, are considered in CASSCF.

Method	J	K	Γ	Γ'
SC	−1.41	0.45	0.55	−0.16
SSCAS	−1.50	0.57	0.47	0.24
CASSCF	−1.30	0.54	0.50	0.21
MRCI	−1.18	0.53	0.51	0.17

Transformed to XXZ frame (see the discussion and conversion relations in SM [22]), the nearest-neighbor MRCI coupling parameters change to $J_{xy} = -1.29$, $J_z = -0.44$, $J_{\pm\pm} = -0.20$, and $J_{z\pm} = -0.09$. Their dependence on the various exchange mechanisms is illustrated in Table III: it is seen that J_{xy} is essentially determined by Coulomb exchange, while for the remaining nearest-neighbor effective interactions, other contributions are also significant, most of all, the dressing with on-site excitations. The relevance of the XXZ effective spin model to the magnetism of $Na_3Co_2SbO_6$ is discussed in Ref. [30].

While the discussion has been focused so far on the pair of edge-sharing CoO_6 octahedra displaying C_{2h} point-group symmetry [21], a similar fine structure is found for the excitation spectrum of the lower-symmetry, C_i Co_2O_{10} unit: the

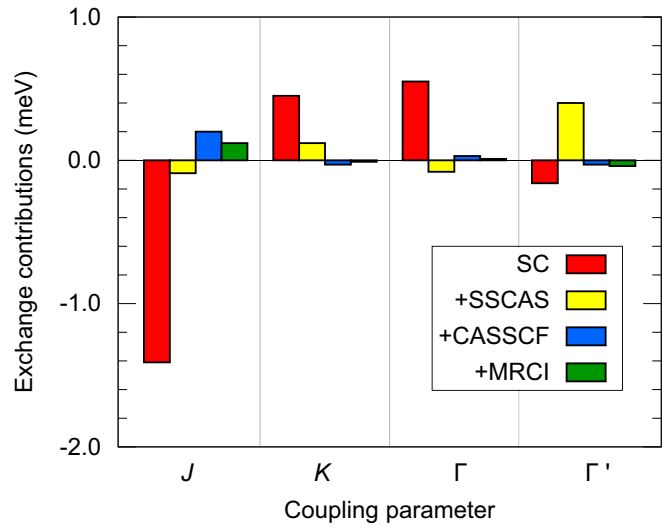


FIG. 2. Direct exchange (red bars), CT kinetic exchange (blue), and CT superexchange plus additional correlation effects (green) in $Na_3Co_2SbO_6$. Yellow bars represent the effect of dressing with on-site excitations. Red and yellow contributions are ignored in the current descriptive exchange models.

TABLE III. Nearest-neighbor effective magnetic couplings (meV) for the C_{2h} Co-Co link [21] in XXZ representation (see SM [22] or, e.g., Ref. [10] for conversion relations).

Method	J_{xy}	J_z	$J_{\pm\pm}$	$J_{z\pm}$
SC	−1.34	−1.11	−0.31	0.12
SSCAS	−1.63	−0.68	−0.17	−0.16
CASSCF	−1.43	−0.51	−0.19	−0.12
MRCI	−1.29	−0.44	−0.20	−0.09

excitation energies of the lowest three excited states (defined by the interaction of the two 1/2 pseudospins) differ on average by 10%. Whether certain details in the experimental spectra can be explained by considering two different sets of Co-Co magnetic links (i.e., two different sets of nearest-, second-, and third-neighbor couplings) remains to be clarified in forthcoming work.

The quantum chemical calculations were limited to adjacent CoO_6 magnetic units and nearest-neighbor K, J, Γ, and Γ' effective couplings. Widely used to study magnetic ground states and excitations on Kitaev-Heisenberg honeycomb lattices are effective spin models augmented with second- and third-neighbor J_2 and J_3 Heisenberg interactions. For $Na_3Co_2SbO_6$, the MRCI nearest-neighbor couplings alone yield ferromagnetic order, and antiferromagnetic longer-ranged Heisenberg exchange ($J_2 \simeq 0.25$, $J_3 \simeq 0.3$, or combinations thereof) is required to tune to a zigzag ground state, in line with the literature and also our own exact-diagonalization calculations. By employing linear spin-wave theory for the K-J-Γ-Γ'-J_2-J_3 model with a classical zigzag ground state, we computed the dynamical structure factor

$$\mathcal{S}^{\perp}(\boldsymbol{Q},\omega) = \sum_{\alpha\beta}\left(\delta_{\alpha\beta} - \frac{Q^{\alpha}Q^{\beta}}{Q^2}\right)\mathcal{S}^{\alpha\beta}(\boldsymbol{Q},\omega), \tag{2}$$

with the matrix elements

$$\mathcal{S}^{\alpha\beta} = \sum_{ij}\int \frac{d\tau}{2\pi} e^{-i\omega\tau}\left\langle S^{\alpha}_{-\boldsymbol{Q}_i}(0) S^{\beta}_{\boldsymbol{Q}_j}(\tau)\right\rangle. \tag{3}$$

Here, $S^{\alpha}_{\boldsymbol{Q}_i}$ is a Fourier-transformed spin operator in the Heisenberg picture, and i, j are lattice sites within the magnetic unit cell. For $Na_3Co_2SbO_6$, the available INS data were measured on powder samples, and we thus considered averaging over all momentum transfer directions. The INS cross section then becomes $\propto F(Q)^2 \int d\Omega \mathcal{S}^{\perp}(\boldsymbol{Q},\omega)$, where $F(Q)$ is the form factor for Co^{2+} [31]. For the given MRCI effective couplings, the best match of the basic INS spectral features was found for $J_2 = 0$ and $J_3 = 0.68$ meV, see Fig. 3; small J_2 contributions would still lead to similar structure factors, but once J_2 reaches the order of J_3, the main features start to differ.

With the exchange parameters used for the plot in Fig. 3, the Curie-Weiss temperature is calculated as $\Theta_{\mathrm{CW}} = -S(S+1)(J + 2J_2 + J_3 + K/3) = 2.8$ K, indicating weak ferromagnetic character. This agrees with the experimentally determined ab-plane averaged $\Theta_{\mathrm{CW}} = 3.9$ K [15,32]. Several comments are in order. While the successful synthesis of single crystals of $Na_3Co_2SbO_6$ was reported [32], corresponding INS data are not available yet—the published INS results

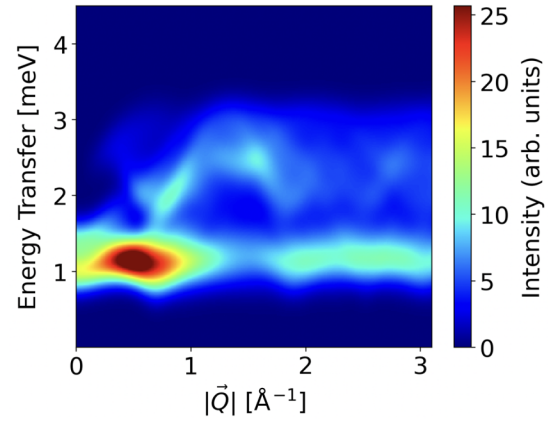


FIG. 3. Powder-averaged dynamical structure factor for $Na_3Co_2SbO_6$. Data were computed within linear spin-wave theory, using the nearest-neighbor MRCI parameters from Table II and $J_3 = 0.68$ meV (details: Gaussian broadening of $\sigma = 0.18$ and intensity cutoff at 5/6 of maximum intensity).

were obtained on polycrystalline samples. What stands out is that all three available experiments [12–14] find strong intensity close to $Q = 0.5$. While a strong signal is also found in our Fig. 3 around $Q = 0.5$, the corresponding energy is lower by roughly 1 meV, and there is less intensity for the branch extending toward $Q \approx 1$. This disagreement remains to be clarified by future work—other effects that need to be addressed are cyclic exchange [30,33–36], additional anisotropies due to the presence of two symmetry-inequivalent sets of Co-Co links on a given hexagonal ring [21], and second-neighbor antisymmetric interactions (allowed by symmetry). That surprisingly small values for the ring-exchange interaction may have a dramatic impact on the magnetic excitation spectra has been recently shown for honeycomb $CoTiO_3$ [36]. As concerns the additional anisotropies due to the presence of two different sets of Co-Co magnetic bonds (i.e., intrinsic uniaxial deformation of the honeycomb lattice that removes C_3 rotation symmetry at the Co sites) [21]: this yields not only two different sets of nearest-, second-, and third-neighbor couplings but also a Γ'' parameter for one set of Co-Co links and a more complicated form of cyclic exchange.

Conclusions. To conclude, analyzing the quantum chemistry of interacting $t_{2g}^5 e_g^2$ magnetic moments, we identify intersite Coulomb exchange and on-site multiconfigurational dressing (red and yellow bars in Fig. 2) as important Kitaev-Heisenberg interaction channels. The Coulomb exchange contributions to K, J, Γ, and Γ' represent firm, assertive results: obtaining those requires computations at the most basic level of approximation in *ab initio* electronic-structure theory, Hartree-Fock-like, different from the much more sophisticated subsequent calculations required to estimate the role of correlations/excitations. Similar results on the magnitude of Coulomb exchange should be obtained by DFT computations with functionals that incorporate exact (i.e., Hartree-Fock) exchange but disregard any correlations. [37] As a comechanism to intersite interactions, both isotropic and anisotropic, Coulomb exchange has already been pointed out in quantum chemical studies of hexagonal d^5 $RuCl_3$ [38] and triangular-lattice d^5 $NaRuO_2$ [38,39]; spotting it as an

important interaction mechanism on a hexagonal d^7 lattice suggests that anisotropic Coulomb exchange is ubiquitous in Kitaev-Heisenberg magnets. Finally, the renormalization of intersite couplings through on-site multiconfigurational dressing is an effect that might also be relevant to, e.g., d^8 NiX_2 nickelates [40].

Acknowledgments. We thank A. Tsirlin, R. C. Morrow, S. L. Drechsler, and M. Richter for discussions, and U. Nitzsche for technical support. P.B., T.P., and L.H. acknowledge financial support from the German Research Foundation (Deutsche Forschungsgemeinschaft, DFG), Project No. 468093414. S.N. acknowledges financial support through the SFB 1143 of the DFG. S.R. acknowledges support by the Australian Research Council (ARC) through Grant No. DP240100168.

Data availability. Research data related to this work have been deposited in the RADAR database under the [52].

[1] A. Kitaev, Anyons in an exactly solved model and beyond, Ann. Phys. (NY) **321**, 2 (2006).
[2] T. Helgaker, P. Jørgensen, and J. Olsen, *Molecular Electronic Structure Theory* (John Wiley & Sons, Chichester, 2000).
[3] P. Fulde, *Correlated Electrons in Quantum Matter* (World Scientific, Singapore, 2012).
[4] G. Khaliullin, Orbital order and fluctuations in Mott insulators, Prog. Theor. Phys. Suppl. **160**, 155 (2005).
[5] G. Jackeli and G. Khaliullin, Mott insulators in the strong spin-orbit coupling limit: From Heisenberg to a quantum compass and Kitaev models, Phys. Rev. Lett. **102**, 017205 (2009).
[6] S. M. Winter, A. A. Tsirlin, M. Daghofer, J. van den Brink, Y. Singh, P. Gegenwart, and R. Valenti, Models and materials for generalized Kitaev magnetism, J. Phys.: Condens. Matter **29**, 493002 (2017).
[7] H. Liu and G. Khaliullin, Pseudospin exchange interactions in d^7 cobalt compounds: Possible realization of the Kitaev model, Phys. Rev. B **97**, 014407 (2018).
[8] H. Liu, J. Chaloupka, and G. Khaliullin, Kitaev spin liquid in 3*d* transition metal compounds, Phys. Rev. Lett. **125**, 047201 (2020).
[9] R. Sano, Y. Kato, and Y. Motome, Kitaev-Heisenberg Hamiltonian for high-spin d^7 Mott insulators, Phys. Rev. B **97**, 014408 (2018).
[10] S. M. Winter, Magnetic couplings in edge-sharing high-spin d^7 compounds, J. Phys. Mater. **5**, 045003 (2022).
[11] X. Liu and H.-Y. Kee, Non-Kitaev versus Kitaev honeycomb cobaltates, Phys. Rev. B **107**, 054420 (2023).
[12] M. Songvilay, J. Robert, S. Petit, J. A. Rodriguez-Rivera, W. D. Ratcliff, F. Damay, V. Balédent, M. Jiménez-Ruiz, P. Lejay, E. Pachoud, A. Hadj-Azzem, V. Simonet, and C. Stock, Kitaev interactions in the Co honeycomb antiferromagnets $Na_3Co_2SbO_6$ and $Na_2Co_2TeO_6$, Phys. Rev. B **102**, 224429 (2020).
[13] C. Kim, J. Jeong, G. Lin, P. Park, T. Masuda, S. Asai, S. Itoh, H.-S. Kim, H. Zhou, J. Ma, and J.-G. Park, Antiferromagnetic Kitaev interaction in $J_{\text{eff}} = 1/2$ cobalt honeycomb materials $Na_3Co_2SbO_6$ and $Na_2Co_2TeO_6$, J. Phys.: Condens. Matter **34**, 045802 (2022).
[14] A. L. Sanders, R. A. Mole, J. Liu, A. J. Brown, D. Yu, C. D. Ling, and S. Rachel, Dominant Kitaev interactions in the honeycomb materials $Na_3Co_2SbO_6$ and $Na_2Co_2TeO_6$, Phys. Rev. B **106**, 014413 (2022).
[15] X. Li, Y. Gu, Y. Chen, V. O. Garlea, K. Iida, K. Kamazawa, Y. Li, G. Deng, Q. Xiao, X. Zheng, Z. Ye, Y. Peng, I. A. Zaliznyak, J. M. Tranquada, and Y. Li, Giant magnetic in-plane anisotropy and competing instabilities in $Na_3Co_2SbO_6$, Phys. Rev. X **12**, 041024 (2022).
[16] M. van Veenendaal, E. H. T. Poldi, L. S. I. Veiga, P. Bencok, G. Fabbris, R. Tartaglia, J. L. McChesney, J. W. Freeland, R. J. Hemley, H. Zheng, J. F. Mitchell, J.-Q. Yan, and D. Haskel, Electronic structure of Co 3*d* states in the Kitaev material candidate honeycomb cobaltate $Na_3Co_2SbO_6$ probed with x-ray dichroism, Phys. Rev. B **107**, 214443 (2023).
[17] L. Hozoi, U. Birkenheuer, H. Stoll, and P. Fulde, Spin-state transition and spin-polaron physics in cobalt oxide perovskites: *ab initio* approach based on quantum chemical methods, New J. Phys. **11**, 023023 (2009).
[18] M. Iakovleva, T. Petersen, A. Alfonsov, Y. Skourski, H.-J. Grafe, E. Vavilova, R. Nath, L. Hozoi, and V. Kataev, Static magnetic and ESR spectroscopic properties of the dimer-chain antiferromagnet $BiCoPO_5$, Phys. Rev. Mater. **6**, 094413 (2022).
[19] C. Albert, T. J. Ballé, F. A. Breitner, Y. Krupskaya, A. Alfonsov, Z. Zangeneh, S. Avdoshenko, M. S. Eldeeb, L. Hozoi, A. Vilangottunjalil, E. Haubold, A. Charnukha, B. Büchner, A. Jesche, and V. Kataev, Terahertz magneto-optical excitations of the sd-hybrid states of lithium nitridocobaltate $Li_2(Li_{1-x}Co_x)N$, Inorg. Chem. **60**, 4497 (2021).
[20] S. Sugano, Y. Tanabe, and H. Kamimura, *Multiplets of Transition-Metal Ions in Crystals* (Academic Press, New York, 1970).
[21] L. Viciu, Q. Huang, E. Morosan, H. Zandbergen, N. Greenbaum, T. McQueen, and R. Cava, Structure and basic magnetic properties of the honeycomb lattice compounds $Na_2Co_2TeO_6$ and $Na_3Co_2SbO_6$, J. Solid State Chem. **180**, 1060 (2007).
[22] See Supplemental Material at http://link.aps.org/supplemental/10.1103/8fz7-9wj9 for detailed information about the numerical calculations, which includes Refs. [2,8,21,23,26,28,29,41–51].
[23] D. A. Kreplin, P. J. Knowles, and H.-J. Werner, MCSCF optimization revisited. II. Combined first- and second-order orbital optimization for large molecules, J. Chem. Phys. **152**, 074102 (2020).
[24] T. Petersen, L. Prodan, K. Geirhos, H. Nakamura, I. Kézsmárki, and L. Hozoi, Dressed j_{eff}-1/2 objects in mixed-valence lacunar spinel molybdates, Sci. Rep. **13**, 2411 (2023).
[25] T. Petersen, P. Bhattacharyya, U. K. Rößler, and L. Hozoi, Resonating holes vs molecular spin-orbit coupled states in group-5 lacunar spinels, Nat. Commun. **14**, 5218 (2023).
[26] P. J. Knowles and H.-J. Werner, Internally contracted multiconfiguration-reference configuration interaction calculations for excited states, Theor. Chim. Acta **84**, 95 (1992).
[27] J. Chaloupka and G. Khaliullin, Hidden symmetries of the extended Kitaev-Heisenberg model: Implications for the

honeycomb-lattice iridates A_2IrO_3, Phys. Rev. B **92**, 024413 (2015).

[28] N. A. Bogdanov, V. M. Katukuri, J. Romhányi, V. Yushankhai, V. Kataev, B. Büchner, J. van den Brink, and L. Hozoi, Orbital reconstruction in nonpolar tetravalent transition-metal oxide layers, Nat. Commun. **6**, 7306 (2015).

[29] R. Yadav, N. A. Bogdanov, V. M. Katukuri, S. Nishimoto, J. van den Brink, and L. Hozoi, Kitaev exchange and field-induced quantum spin-liquid states in honeycomb α-$RuCl_3$, Sci. Rep. **6**, 37925 (2016).

[30] Y. Gu, X. Li, Y. Chen, K. Iida, A. Nakao, K. Munakata, V. O. Garlea, Y. Li, G. Deng, I. A. Zaliznyak, J. M. Tranquada, and Y. Li, In-plane multi-q magnetic ground state of $Na_3Co_2SbO_6$, Phys. Rev. B **109**, L060410 (2024).

[31] R. E. Watson and A. J. Freeman, Hartree-Fock atomic scattering factors for the iron transition series, Acta. Cryst. **14**, 27 (1961).

[32] J.-Q. Yan, S. Okamoto, Y. Wu, Q. Zheng, H. D. Zhou, H. B. Cao, and M. A. McGuire, Magnetic order in single crystals of $Na_3Co_2SbO_6$ with a honeycomb arrangement of $3d^7Co^{2+}$ ions, Phys. Rev. Mater. **3**, 074405 (2019).

[33] W. G. F. Krüger, W. Chen, X. Jin, Y. Li, and L. Janssen, Triple-q order in $Na_2Co_2TeO_6$ from proximity to hidden-SU(2)-symmetric point, Phys. Rev. Lett. **131**, 146702 (2023).

[34] N. Francini and L. Janssen, Spin vestigial orders in extended Heisenberg-Kitaev models near hidden SU(2) points: Application to $Na_2Co_2TeO_6$, Phys. Rev. B **109**, 075104 (2024).

[35] Y. Gu, X. Jin, and Y. Li, On the multi-q characteristics of magnetic ground states of honeycomb cobalt oxides, Chinese Phys. Lett. **42**, 027303 (2025).

[36] Y. Li, T. T. Mai, M. Karaki, E. V. Jasper, K. F. Garrity, C. Lyon, D. Shaw, T. DeLazzer, A. J. Biacchi, R. L. Dally, D. M. Heligman, J. Gdanski, T. Adel, M. F. Muñoz, A. Giovannone, A. Pawbake, C. Faugeras, J. R. Simpson, K. Ross, N. Trivedi, *et al.*, Ring-exchange interaction effects on magnons in the Dirac magnet $CoTiO_3$, Phys. Rev. B **109**, 184436 (2024).

[37] Describing kinetic exchange and superexchange (i.e., intersite *excitations*) through the (exchange-)correlation functional remains, however, elusive.

[38] P. Bhattacharyya, T. Petersen, N. A. Bogdanov, and L. Hozoi, Coulomb exchange as source of Kitaev and off-diagonal symmetric anisotropic couplings, Commun. Phys. **7**, 121 (2024).

[39] P. Bhattacharyya, N. A. Bogdanov, S. Nishimoto, S. D. Wilson, and L. Hozoi, $NaRuO_2$: Kitaev-Heisenberg exchange in triangular-lattice setting, npj Quantum Mater. **8**, 52 (2023).

[40] P. P. Stavropoulos, D. Pereira, and H.-Y. Kee, Microscopic mechanism for a higher-spin Kitaev model, Phys. Rev. Lett. **123**, 037203 (2019).

[41] H.-J. Werner, P. J. Knowles, G. Knizia, F. R. Manby, and M. Schütz, Molpro: A general-purpose quantum chemistry program package, WIREs Comput. Mol. Sci. **2**, 242 (2012).

[42] M. Klintenberg, S. Derenzo, and M. Weber, Accurate crystal fields for embedded cluster calculations, Comput. Phys. Commun. **131**, 120 (2000).

[43] S. E. Derenzo, M. K. Klintenberg, and M. J. Weber, Determining point charge arrays that produce accurate ionic crystal fields for atomic cluster calculations, J. Chem. Phys. **112**, 2074 (2000).

[44] A. Berning, M. Schweizer, H.-J. Werner, P. J. Knowles, and P. Palmieri, Spin-orbit matrix elements for internally contracted multireference configuration interaction wavefunctions, Mol. Phys. **98**, 1823 (2000).

[45] N. B. Balabanov and K. A. Peterson, Systematically convergent basis sets for transition metals. I. All-electron correlation consistent basis sets for the 3*d* elements Sc-Zn, J. Chem. Phys. **123**, 064107 (2005).

[46] T. H. Dunning, Gaussian basis sets for use in correlated molecular calculations. I. The atoms boron through neon and hydrogen, J. Chem. Phys. **90**, 1007 (1989).

[47] F. Schautz, H.-J. Flad, and M. Dolg, Quantum Monte Carlo study of Be_2 and group 12 dimers M2 (M = Zn, Cd, Hg), Theor. Chem. Acc. **99**, 231 (1998).

[48] H. Stoll, B. Metz, and M. Dolg, Relativistic energy-consistent pseudopotentials—Recent developments, J. Comput. Chem. **23**, 767 (2002).

[49] K. Pierloot, B. Dumez, P.-O. Widmark, and B. O. Roos, Density matrix averaged atomic natural orbital (ANO) basis sets for correlated molecular wave functions, Theor. Chim. Acta **90**, 87 (1995).

[50] P. Fuentealba, H. Preuss, H. Stoll, and L. Von Szentpály, A proper account of core-polarization with pseudopotentials: single valence-electron alkali compounds, Chem. Phys. Lett. **89**, 418 (1982).

[51] J. Pipek and P. G. Mezey, A fast intrinsic localization procedure applicable for *ab initio* and semiempirical linear combination of atomic orbital wave functions, J. Chem. Phys. **90**, 4916 (1989).

[52] P. Bhattacharyya, Kitaev-Heisenberg exchange on $t_{2g}^5 e_g^2$ cobaltate platform, Leibniz Institute for Solid State and Materials Research (2025), doi:10.22000/tny338gct87gzce4.